

Andreev drag effect in ferromagnetic-normal-superconducting systems

David Sánchez, Rosa López, Peter Samuelsson, and Markus Büttiker

Département de Physique Théorique, Université de Genève, CH-1211 Genève 4, Switzerland

(Dated: September 27, 2018)

We investigate conductances and current correlations in a system consisting of a normal multichannel conductor connected to one superconducting and two ferromagnetic electrodes. For antiparallel orientation of the ferromagnet polarizations, current injection from one ferromagnet can, due to Andreev reflection, lead to a net drag of current from the second ferromagnet toward the superconductor. We present the conditions for the Andreev drag in terms of lead polarizations, contact conductances and spin-flip scattering. Remarkably, both equilibrium and nonequilibrium zero-frequency current correlations between the ferromagnets become positive even in the presence of spin relaxation.

PACS numbers: 74.45.+c 72.25.-b 72.70.+m

I. INTRODUCTION

At a normal-superconducting interface, Andreev reflection causes a conversion of the quasiparticle charge *and* a flipping of its spin—an electron with spin up, incoming towards the superconductor, is reflected as a hole with spin down. This leads to exciting consequences in the transport physics where the focus is put on creating, manipulating and detecting spin currents and magnetization.^{1,2} When the carriers are spin polarized, the transport properties are strongly sensitive to the relative orientation of the ordered moments of ferromagnetic electrodes,^{3,4} a feature that has received a lot of interest due to the relatively long spin dephasing times observed in metals^{5,6} and semiconductors.⁷ In hybrid systems containing a superconductor, various aspects of the interplay between Andreev reflection and ferromagnetism have been addressed theoretically^{8,9} and experimentally.^{10,11,12}

The structure of interest here is shown in Fig. 1(a): two ferromagnetic contacts are connected to a normal conductor which is in turn connected to a superconductor. Of particular interest is the case of crossed Andreev reflection between ferromagnetic leads with antiparallel polarization dominating over crossed normal reflection. In such a geometry, with a voltage applied to one of the leads while the other lead and the superconductor are grounded, the injected current from the biased ferromagnetic lead effectively *drags* along a current from the grounded lead. This effect is easy to understand since the transfer of Cooper pairs into the superconductor requires a pair of electrons with opposite spin. If the injected current consists only of, say, spin-up carriers, the system supplies the spin-down carriers from the oppositely polarized ferromagnetic lead even though no voltage is applied at this contact.

The physics of the Andreev drag effect was already addressed by Jedema and van Wees *et al.*¹³ for a multi-terminal metallic diffusive conductor. These authors pointed to negative four-terminal resistances as a consequence of the Andreev drag effect. In contrast, much of the recent theoretical discussion has focused on a geom-

etry where two needle-shaped ferromagnetic leads with antiparallel polarization are directly coupled to a superconductor at two spatially separated points.¹⁴ In this case, even in the case of 100% spin polarization, the crossed Andreev reflection probability is strongly suppressed in realistic geometries,¹⁵ making the experimental detection of the drag effect difficult. In addition, the direct connection of the ferromagnetic electrodes to the superconductor might lead to unwanted modifications of the local properties of the ferromagnet¹¹ and the superconductor,¹² suppressing the drag effect.

In this work, we overcome the above difficulties by inserting a normal multichannel¹⁶ mesoscopic conductor with generic elastic scattering between the ferromagnetic electrodes and the superconductor [see the sketch of Fig. 1(a)]. We include arbitrary interface conductances and spin-flip relaxation (see below). The advantage of this scheme is twofold: (i) since the superconductor is only contacted at one point, the drag effect develops to the fullest extent possible, being of the order of the conductances of the contacts between the

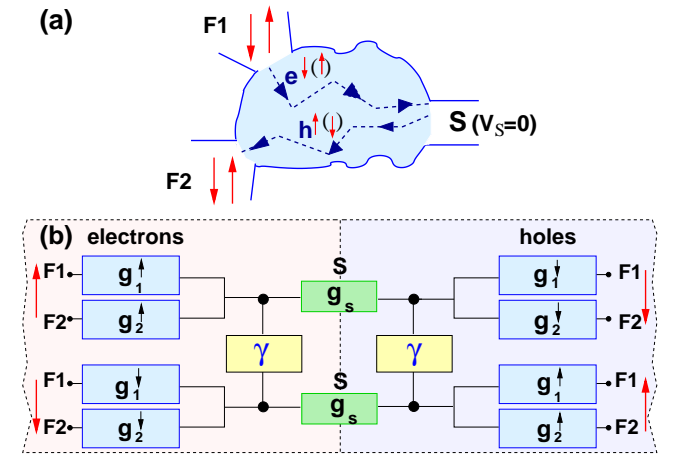


FIG. 1: (a) Generic ferromagnetic-normal-superconducting structure: the process that gives rise to the Andreev drag effect is indicated. (b) Sketch of the equivalent circuit model (see text).

normal conductor and the ferromagnetic and superconducting electrodes; and (ii) the sources of the competing phenomena—superconductivity and ferromagnetism—are spatially separated by the normal conductor.

We find that the Andreev drag effect is observable when the conductance of the normal-superconducting (NS) interface dominates over the ferromagnetic-normal (FN) contact conductances. The drag effect is reinforced with increasing lead polarization and survives for a considerable amount of spin-flip scattering. Furthermore, we demonstrate that the crossed Andreev reflections have a profound influence on the zero-frequency current-current cross-correlations. We observe that both the thermal noise and the shot noise power measured between the two ferromagnetic leads yield *positive* values.

II. MODEL

We analyze a hybrid system (shown in Fig. 1) consisting of a normal conductor connected to two ferromagnetic (F1 and F2) and one superconducting (S) reservoirs. For simplicity, the direction of the magnetization of the two ferromagnets is assumed to be collinear and we consider identical FN couplings. Any type of contacts, e.g. diffusive-, ballistic- or tunnel contacts, can be treated. In what follows, we deal with point contacts at the FN (NS) interface with N (M) transversal modes and mode independent transparency Γ (Γ_S). We consider the case with dimensionless conductances (in units of $2e^2/h$) much larger than unity: $g = N\Gamma$, $g_S = MR \gg 1$, where $R = \Gamma_S^2/(2 - \Gamma_S)^2$ is the Andreev reflection probability. Under these conditions, weak localization as well as Coulomb blockade effects can be safely neglected. Moreover, the dwell time of the normal conductor, τ_d , is assumed to be shorter than typical inelastic scattering times.

Throughout the paper, we consider the case when the proximity effect inside the normal conductor is suppressed (but the Andreev reflection at the NS interface is taken into account). A strong proximity effect would quench the drag effect as the normal conductor would behave effectively as a superconductor.¹⁷ This can be avoided either with a magnetic field (e.g., a stray field from the ferromagnets or an externally applied field) or with a characteristic quasiparticle energy (bias eV or temperature $k_B T$) much larger than the inverse dwell time, $eV, k_B T \gg \hbar/\tau_d$. Nevertheless, to avoid single particle transport, both eV and $k_B T$ should be smaller than the gap of the superconductor.

The resistance of the system is completely dominated by the resistances of the FN and NS contacts. Moreover, we assume that the physical properties within the conductor are isotropic due to diffusive or chaotic scattering. We can thus consider the normal conductor to be effectively zero dimensional. This restricts our model to systems with a spin-flip length much larger than the lateral dimensions of the system, i.e., there are no spatial

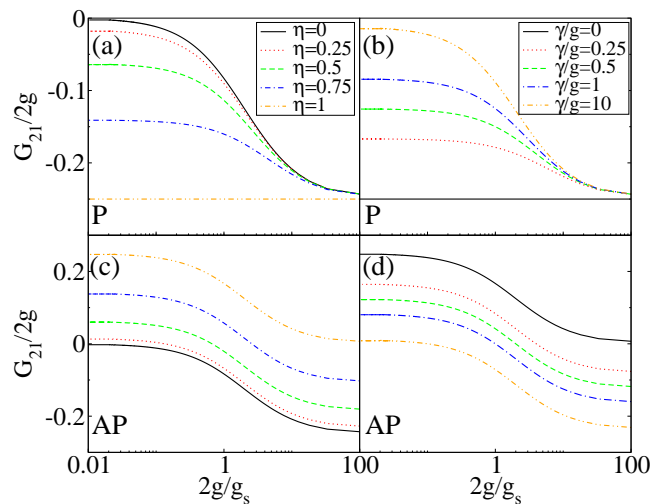


FIG. 2: Off-diagonal conductance $G_{21} = (h/2e^2)\mathcal{I}_2/V_1$ of the current in ferromagnetic lead F2 when a voltage bias is applied to lead F1 as a function of the contact conductances. The magnetic moments of the reservoirs are aligned parallel in (a) with spin-flip rate $\gamma = 0$ and (b) with polarization $\eta = 1$. (c) and (d) same as (a) and (b) in the antiparallel orientation.

variations of accumulated spins inside the dot, though no assumptions are made about the relation between the spin-flip time τ_{sf} and τ_d . We stress that all the above constraints form a situation that is experimentally accessible with present techniques. Vertical structures like metallic thin-film heterostructures, epitaxial layers of half-metallic chromium dioxide or diluted magnetic semiconductors are equally suitable for the observation of the effects discussed here. In fact, a uniform spin accumulation was very recently achieved in a normal metallic island coupled to magnetic leads.¹⁸

General theoretical formulations of semiclassical spin transport, based on quasiclassical Green's functions, have been developed by Brataas, Nazarov and Bauer for normal-ferromagnetic systems¹⁹ and by Belzig *et al.* for normal-ferromagnetic-superconducting systems.⁹ Here, we follow the approach of Samuelsson and Büttiker²⁰ extended to spin-dependent transport. This simple theory is equivalent to Refs. 9,19 for the geometry in Fig 1(a). It is directly formulated in terms of distribution functions and allows us to treat the current and the current correlations within a unified framework. Because the proximity effect is suppressed, the electrons and holes are independent²⁰ and the system is mapped onto the equivalent circuit of Fig. 1(b) in which the electron and hole subsystems (with opposite spins) are connected via Andreev reflection. Spin relaxation in the normal conductor gives rise to a spin-flip current between the spin subsystems with the same quasiparticle charge. As a result, we can describe the conductor with four nodes [two nodes (\uparrow and \downarrow) for each quasiparticle type (electrons and holes)] connected to each other and to the ferromagnetic reservoirs via spin dependent resistances. We model

the spin dependent conductances of the FN contacts as $g_{\alpha}^{\uparrow\downarrow} = g(1 \pm \eta_{\alpha})/2$, where η_{α} is the spin polarization of the lead α ($\alpha = \{1, 2\}$): $\eta_{\alpha} = (\nu_{\alpha}^{\uparrow} - \nu_{\alpha}^{\downarrow})/(\nu_{\alpha}^{\uparrow} + \nu_{\alpha}^{\downarrow})$, where ν_{α}^{σ} is the density of states of the ferromagnetic lead close to the Fermi energy ($\sigma = \{\uparrow, \downarrow\}$).

Conservation of time-averaged (spin-dependent) current densities must be fulfilled at each node for every energy E . Currents flowing into the normal conductor are defined positive such that the *spectral* currents obey

$$\sum_{\alpha} i_{\alpha q}^{\uparrow} \mp i_S^{\uparrow} + i_{\downarrow\uparrow, e} = 0, \quad \sum_{\alpha} i_{\alpha q}^{\downarrow} \mp i_S^{\downarrow} - i_{\downarrow\uparrow, e} = 0, \quad (1)$$

where $q = (e, h)$ labels the carrier (electron or hole) and $- (+)$ is for $q = e$ ($q = h$). The currents through the FN and NS contacts are:

$$i_{\alpha q}^{\sigma} = g_{\alpha q}^{\sigma}(f_{\alpha q} - \hat{f}_q^{\sigma}), \quad i_S^{\sigma} = g_S(\hat{f}_e^{\sigma} - \hat{f}_h^{\sigma})/2, \quad (2)$$

where $f_{\alpha q}(E) = \{1 + \exp([E \mp eV_{\alpha}]/kT)\}^{-1}$ is the equilibrium distribution function at reservoir α . Note that $f_{\alpha q}$ is spin independent as spin relaxation mechanisms are usually highly efficient in ferromagnets. In Eq. (2), $\hat{f}_q^{\sigma}(E)$ is the nonequilibrium distribution function of the normal conductor to be calculated from Eq. (1). The spin-flip current $i_{\downarrow\uparrow, q} = \gamma(\hat{f}_q^{\downarrow} - \hat{f}_q^{\uparrow})$ equilibrates the spin distributions. Here, $\gamma = h\nu_0/\tau_{\text{sf}}$ (ν_0 is the density of states of the conductor at the Fermi energy and τ_{sf} the spin-flip time).¹⁹

III. CONDUCTANCE MATRIX

The *total* current flowing out of reservoir α is

$$\mathcal{I}_{\alpha} = \mathcal{I}_{\alpha e}^{\uparrow} + \mathcal{I}_{\alpha e}^{\downarrow} - \mathcal{I}_{\alpha h}^{\uparrow} - \mathcal{I}_{\alpha h}^{\downarrow}, \quad (3)$$

where $\mathcal{I}_{\alpha q}^{\sigma} = (e/h) \int dE i_{\alpha q}^{\sigma}(E)$, from which we determine the conductance matrix. The conductance $G_{\alpha\beta}$ relates the current \mathcal{I}_{α} with a voltage change at lead β . In the case $V_1 > 0$ and $V_2 = V_S = 0$, the interesting conductance is $G_{21} = (h/2e^2)(\mathcal{I}_2/V_1)$:

$$G_{21} = \frac{g^2[g(\eta_1^2 + \eta_2^2 - 2) - 4\gamma - 2\eta_1\eta_2g_S]}{g^2[4 - (\eta_1 + \eta_2)^2] + 8\gamma g_S + 4g(2\gamma + g_S)}. \quad (4)$$

In a normal system, G_{21} is always negative.²¹ On the contrary, in our system we can have $G_{21} > 0$, which is the manifestation of the Andreev drag effect.²² Figure 2 shows the behavior of G_{21} as a function of $2g/g_S$. In the parallel (P) case, $\eta_1 = \eta_2 = \eta$ and G_{21} is negative [Fig. 2(a)]. The maximum (absolute) value of G_{21} is attained at $\eta = 1$ and decreases with increasing values of γ [Fig. 2(b)]. In the antiparallel (AP) configuration ($\eta_1 = -\eta_2 = \eta$), a *reversal* of the current at F2 occurs for low values of g/g_S and γ [see Fig. 2(c) and Fig. 2(d)]. Note that the drag effect can result already for a small value of η . In fact, crossed Andreev reflections start to dominate when $\eta^2 > (g/g_S)/(1 + g/g_S)$ at $\gamma = 0$. In

particular, for the fully polarized case one always finds $G_{21} > 0$ *regardless of the ratio g/g_S* . When $g_S \gg g$, we find that $G_{21} > 0$ holds for any value of $\eta > 0$, in agreement with Ref. 13. Increasing γ , the spin relaxation processes randomize the spin distributions and eventually lead to $G_{21} < 0$, [the curves tend to the $\eta = 0$ case of Fig. 2(b)]. The condition for the drag effect is:

$$2\gamma < \eta^2 g_S - g(1 - \eta^2). \quad (5)$$

This is a central result of our work.

Interestingly, the Andreev drag effect implies that even the equilibrium Nyquist-Johnson noise yields *positive* current cross-correlations $P_{21} = 4k_B T G_{21}$ in contrast to normal conductors. Nevertheless, energy dissipation is ensured as the eigenvalues of the conductance matrix are semipositive.

Another striking result is that for $\eta = 1$ there are two linearly independent voltage configurations that yield *zero* eigenvalue of the conductance matrix. One is the gauge solution ($V_1 = V_2 = V_S$). The nontrivial arrangement is $V_1 = -V_2 = V$ and $V_S = 0$. Here, F1 injects electrons whereas an equivalent flow of incident holes stems from F2. Complete Andreev reflection yields then zero net current.

IV. MAGNETIZATION

Out of equilibrium for $V_1 > 0$ and $V_2 = V_S = 0$, an accumulation of majority spins forms within the conductor. Before applying the voltage, the conductor has zero magnetization. In the AP case, the polarization excess is given by

$$M = \frac{\int dE \sum_q (\hat{f}_q^{\uparrow} - \hat{f}_q^{\downarrow})}{\int dE \sum_q (\hat{f}_q^{\uparrow} + \hat{f}_q^{\downarrow})} = \frac{g\eta}{2\gamma + g + g_S}. \quad (6)$$

It approaches η for $g \gg g_S, \gamma$ and vanishes for $\gamma \gg g$ or $g_S \gg g$.

V. CROSS CORRELATIONS

To obtain additional insight into the drag effect, we investigate the shot noise of the current. Of particular interest are the correlations between currents flowing in the two ferromagnetic reservoirs. In purely normal systems, the current cross-correlations are manifestly negative.²³ However, in hybrid superconducting structures it was shown that Andreev reflections can cause a reversal of the sign of the cross-correlations.²⁴ The positive correlations in few-mode conductors were also shown to be enhanced by ferromagnetic leads.²⁵ Here, we focus on the cross correlations in the AP configuration, which is the most interesting case.

The contacts act as generators of fluctuations $\delta i_{\alpha q}^{\sigma}$ and δi_S^{σ} . As a result, the spin-dependent distribution function of the normal conductor fluctuates itself. The total

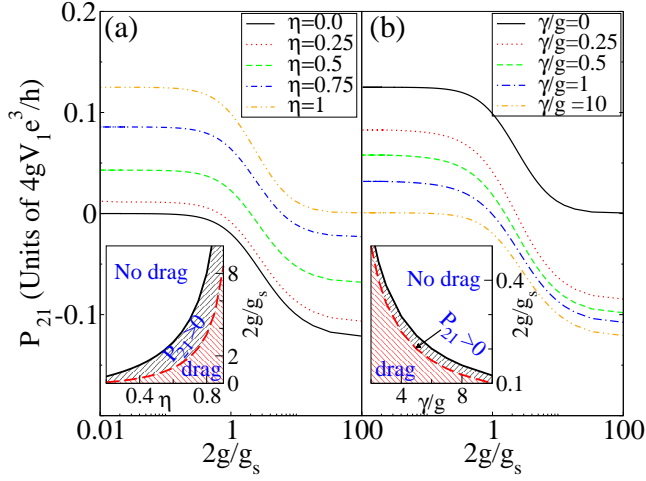


FIG. 3: Cross correlation P_{12} for $\Gamma = 1$ and $R = 1$ versus the ratio of the conductances of the point contacts in the antiparallel case. In (a) $\gamma = 0$ whereas in (b) $\eta = 1$. Insets: “Phase diagram” of the occurrence of the Andreev drag effect (below the dashed line) and positive P_{12} (below the solid line) for (a) $\gamma = 0$ and (b) $\eta = 1$.

fluctuating current is

$$\Delta i_{\alpha q}^{\sigma} = \delta i_{\alpha q}^{\sigma} - g_{\alpha}^{\sigma} \delta \hat{f}_q^{\sigma}, \quad \Delta i_S^{\sigma} = \delta i_S^{\sigma} + g_S (\delta \hat{f}_e^{\bar{\sigma}} - \delta \hat{f}_h^{\sigma}). \quad (7)$$

We also take into account the fluctuations $\delta i_{\downarrow \uparrow, q}$ due to spin relaxation, giving the fluctuating current

$$\Delta i_{\downarrow \uparrow, q} = \delta i_{\downarrow \uparrow, q} + \gamma (\delta \hat{f}_q^{\downarrow} - \delta \hat{f}_q^{\uparrow}). \quad (8)$$

The next step is to determine the fluctuations of the distribution functions of the conductor, $\delta \hat{f}_q^{\sigma}$. In the zero frequency limit, the fluctuating currents are conserved (\mp for $q = e, h$):

$$\sum_{\alpha} \Delta i_{\alpha q}^{\uparrow} \mp \Delta i_S^{\uparrow} + \Delta i_{\downarrow \uparrow, q} = 0, \quad (9a)$$

$$\sum_{\alpha} \Delta i_{\alpha q}^{\downarrow} \mp \Delta i_S^{\downarrow} - \Delta i_{\downarrow \uparrow, q} = 0. \quad (9b)$$

The fluctuations of the charge current at contact α are found from $\Delta i_{\alpha} = \Delta i_{\alpha e}^{\uparrow} + \Delta i_{\alpha e}^{\downarrow} - \Delta i_{\alpha h}^{\uparrow} - \Delta i_{\alpha h}^{\downarrow}$.

The noise power of the current cross-correlations is

$$P_{21} = 2 \int dt \langle \Delta \mathcal{I}_2(t) \Delta \mathcal{I}_1(0) \rangle. \quad (10)$$

The contacts emit fluctuations independently so that

$$\langle \delta i_{\alpha q}^{\sigma}(E, t) \delta i_{\alpha' q'}^{\sigma'}(E', t') \rangle = \frac{\hbar}{e} \bar{\delta} S_{\alpha q}^{\sigma}, \quad (11)$$

with $\bar{\delta} \equiv \delta_{\alpha \alpha'} \delta_{q q'} \delta_{\sigma \sigma'} \delta(E - E') \delta(t - t')$. Here, $S_{\alpha q}^{\sigma}$ is the fluctuation power:^{20,23}

$$S_{\alpha q}^{\sigma} = e g_{\alpha}^{\sigma} [f_{\alpha q}^{\sigma} + \hat{f}_q^{\sigma} - 2 \hat{f}_q^{\sigma} f_{\alpha q}^{\sigma} - \Gamma (f_{\alpha q}^{\sigma} - \hat{f}_q^{\sigma})^2], \quad (12a)$$

$$S_S^{\sigma} = e g_S [\hat{f}_e^{\sigma} + \hat{f}_h^{\bar{\sigma}} - 2 \hat{f}_h^{\bar{\sigma}} \hat{f}_e^{\sigma} - R (\hat{f}_e^{\sigma} - \hat{f}_h^{\bar{\sigma}})^2] / 2, \quad (12b)$$

$$S_{\downarrow \uparrow q} = e \gamma [\hat{f}_q^{\downarrow} + \hat{f}_q^{\uparrow} - 2 \hat{f}_q^{\uparrow} \hat{f}_q^{\downarrow}], \quad (12c)$$

where we have assumed that the statistics of spin-flip events is Poissonian.²⁶

The above system of equations is complete and can be solved for any set of applied voltages, polarization alignments and spin-flip rates. We calculate P_{21} for the bias configuration given by $V_1 > 0$, $V_2 = V_S = 0$ in the AP case at $k_B T = 0$. We present only the analytical result in limiting cases and show the general result in Fig. 3. In Fig. 3(a), we plot P_{21} as a function of the conductance ratio $2g/g_S$ for various polarizations η , $\gamma = 0$ and $\Gamma = R = 1$. (Qualitatively, the results are independent of Γ and R .) For $\eta = 0$, the cross-correlations are negative. As η is turned on, P_{21} can become positive. With increasing g/g_S , P_{21} exhibits a crossover from negative to positive values at $2g/g_S \sim 1$. Indeed, for dominating NS conductance (small g/g_S) we find

$$P_{21} = p_0 \eta^2 [\Gamma + 2 - \eta^2 (3\Gamma - 2)] / 16 + \mathcal{O}(g/g_S), \quad (13)$$

which is manifestly positive for $\eta > 0$ ($p_0 \equiv 4gV_1 e^3/h$). In this case, the electron and hole distributions within the conductor are almost identical.

On the other hand, for dominating FN conductance (small g_S/g) the cross-correlations become

$$P_{21} = p_0 (1 - \eta^2) [\Gamma - 2 + \eta^2 (3\Gamma - 2)] / 8 + \mathcal{O}(g_S/g), \quad (14)$$

which are negative for $\eta < 1$. Notice that for $\eta = 0$ this expression yields the shot noise for a chaotic dot coupled to two normal leads. In the fully polarized case, the cross-correlations are *always* positive independently of g/g_S .

For illustrative purposes we show in the inset of Fig. 3(a) the “phase diagram” ($\eta, g/g_S$). The solid line marks the crossover between positive and negative cross-correlations. With increasing η , the crossover point shifts toward larger values of $2g/g_S$. For comparison, we also plot a dashed curve that marks the transition to the Andreev drag effect. Notice that the conditions $P_{21} > 0$ and $G_{21} > 0$ are closely related, but not identical. This is the case since the scattering processes in general contribute in different ways for the current and noise.²⁰

A finite source of spin relaxation leads to the suppression of positive P_{21} . To see this, we show in Fig. 3(b) the cross-correlations for the fully polarized case for different values of γ . For nonzero values of γ , P_{21} becomes negative with increasing $2g/g_S$. Eventually, when $\gamma \rightarrow \infty$, we recover the unpolarized case ($\eta = 0$) of Fig. 3(a).

VI. CONCLUSIONS

We have investigated the transport properties of a normal conductor attached to ferromagnetic leads and coupled to a superconductor in the subgap regime. The proposed geometry, which includes generic elastic and spin-flip scattering, is shown to exhibit a pronounced Andreev drag effect. We have demonstrated that the equilibrium and transport current correlations are strongly sensitive

to crossed Andreev reflections. The theory presented here applies to a wide range of geometries and should therefore advance experimental observation of the Andreev drag effect.

Note added in proof. Recently, we became aware of the work of Lambert *et al.*²⁷ who compute numerically the conductances for a metallic diffusive geometry similar to Fig. 1. They also conclude that a normal conductor inserted between the ferromagnetic and the superconducting contacts leads to an enhancement of the Andreev drag effect. In contrast to our work, the role of spin-flip, the effect of differing lead polarizations, and the shot noise

are not investigated.

Acknowledgments

We thank V. Chandrasekhar and B.J. van Wees for helpful discussions. We acknowledge support from the Swiss NSF through the program MANEP. D.S. and R.L. were also supported by the EU RTN under Contract No. HPRN-CT-2000-00144, Nanoscale Dynamics.

-
- ¹ See, e.g., S.A. Wolf, D.D. Awschalom, R.A. Buhrman, J.M. Daughton, S. von Molnár, M.L. Roukes, A.Y. Chtchelkanova, and D.M. Treger, *Science* **294**, 1488 (2001) and references therein.
- ² R. Fiederling, M. Keim, G. Reuscher, W. Ossau, G. Schmidt, A. Waag, and L. W. Molenkamp, *Nature (London)* **402**, 787 (1999); Y. Ohno, D.K. Young, B. Beschoten, F. Matsukura, H. Ohno, and D.D. Awschalom **402**, 790 (1999).
- ³ M.N. Baibich, J.M. Broto, A. Fert, F. Nguyen Van Dau, F. Petroff, P. Eitenne, G. Creuzet, A. Friederich, and J.C. Chazelas, *Phys. Rev. Lett.* **61**, 2472 (1988).
- ⁴ J.C. Slonczewski, *Phys. Rev. B* **39**, 6995 (1989).
- ⁵ M. Johnson and R.H. Silsbee, *Phys. Rev. Lett.* **55**, 1790 (1985).
- ⁶ F.J. Jedema, A.T. Filip and B.J. van Wees, *Nature (London)* **410**, 345 (2001).
- ⁷ J.M. Kikkawa, I.P. Smorchkova, N. Samarth, and D. D. Awschalom, *Science* **281**, 1284 (1997).
- ⁸ M.J.M de Jong, and C.W.J. Beenakker, *Phys. Rev. Lett.* **74**, 1657 (1995); V.I. Fal'ko, A.F. Volkov, and C. Lambert, *Phys. Rev. B* **60**, 15 394 (1999); S. Takahashi, H. Imamura, and S. Maekawa, *Phys. Rev. Lett.* **82**, 3911 (1999); D. Huertas-Hernando, Yu.V. Nazarov, and W. Belzig, *Phys. Rev. Lett.* **88**, 047003 (2002).
- ⁹ W. Belzig, A. Brataas, Yu.V. Nazarov, and G.E.W. Bauer, *Phys. Rev. B* **62**, 9726 (2000).
- ¹⁰ M.D. Lawrence and N. Giordano, *J. Phys. Condens. Matter* **8**, L563 (1996); M. Giroud, H. Courtois, K. Hasselbach, D. Mailly, and B. Pannetier, *Phys. Rev. B* **58**, 11 872 (1998); S.K. Upadhyay, A. Palanisami, R.N. Louie, and R.A. Buhrman, *Phys. Rev. Lett.* **81**, 3247 (1998); R.J. Soulen Jr., J.M. Byers, M.S. Osofsky, B. Nadgorny, T. Ambrose, S.F. Cheng, P.R. Broussard, C.T. Tanaka, J. Nowak, J.S. Moodera, A. Barry, and J.M.D. Coey, *Science* **282**, 85 (1998).
- ¹¹ J. Aumentado and V. Chandrasekhar, *Phys. Rev. B* **64**, 054505 (2000); S.V. Dubonos, A.K. Geim, K.S. Novoselov, and I.V. Grigorieva, *ibid* **65**, 220513 (2002).
- ¹² V.T. Petrashov, I.A. Sosnin, I. Cox, A. Parsons, and C. Troadec, *Phys. Rev. Lett.* **83**, 3281 (1999).
- ¹³ F.J. Jedema, B.J. van Wees, B.H. Hoving, A.T. Filip, and T.M. Klapwijk, *Phys. Rev. B* **60**, 16 549 (1999).
- ¹⁴ G. Deutscher and D. Feinberg, *Appl. Phys. Lett.* **76**, 487 (2000); G. Falci, D. Feinberg, and F.W.J. Hekking, *Europhys. Lett.* **54**, 255 (2001).
- ¹⁵ M.-S. Choi, C. Bruder, and D. Loss, *Phys. Rev. B* **62**, 13 569 (2000); P. Recher, E.V. Sukhorukov, and D. Loss, *ibid.* **63**, 165314 (2000).
- ¹⁶ A drag effect in a single-mode conductor in the absence of spin flip scattering has been pointed out in G. Lesovik, Th. Martin, and G. Blatter, *Euro. Phys. J. B* **24**, 287 (2001). A single quantum level is considered by Y. Zhu, Q.F. Sun, and T.H. Lin, *Phys. Rev. B* **65**, 024516 (2001).
- ¹⁷ We are then back to the situation of Ref. 14.
- ¹⁸ M. Zaffalon and B.J. van Wees, *Phys. Rev. Lett.* **91**, 186601 (2003).
- ¹⁹ A. Brataas, Yu.V. Nazarov, and G.E.W. Bauer, *Phys. Rev. Lett.* **84**, 2481 (2000); *Euro. Phys. J. B* **22**, 99 (2001).
- ²⁰ P. Samuelsson and M. Büttiker, *Phys. Rev. B* **66**, 201306 (2002).
- ²¹ M. Büttiker, *Phys. Rev. Lett.* **57**, 1761 (1986).
- ²² In a normal system, injection of current into contact α causes out-flowing currents in contact $\beta \neq \alpha$, resulting in negative off-diagonal conductance, see Ref. 21. In contrast, for interacting systems off-diagonal conductances can be positive. See C.C. Chamon and E. Fradkin, *Phys. Rev. B* **56**, 2012 (1997) and K.-V. Pham, F. Piechon, K.-I. Imura, and P. Lederer, cond-mat/0207294 (unpublished). A discussion of the signs of the conductance matrix elements in NS-structures without ferromagnets is given by N.K. Allsopp, V.C. Hui, C.J. Lambert, and S.J. Robinson, *J. Phys.: Condens. Matter* **6**, 10 475 (1994). See also the focusing experiments; S.I. Bozkom, V.S. Tsoi, and S.E. Yakovlev, *Pis'ma Zh. Eksp. Teor. Fiz.* **36**, 123 (1982) [*JETP Lett.* **36**, 153 (1982)]; P.A.M. Benistant, H. van Kampen, and P. Wyder, *Phys. Rev. Lett.* **51**, 817 (1983).
- ²³ M. Büttiker, *Phys. Rev. B* **46**, 12485 (1992).
- ²⁴ M.P. Anantram and S. Datta, *Phys. Rev. B* **53**, 16 390 (1996); J. Torres and T. Martin, *Eur. Phys. J. B.* **12**, 319 (1999); T. Gramspacher and M. Büttiker, *Phys. Rev. B* **61**, 8125 (2000); J. Börlin, W. Belzig, and C. Bruder, *Phys. Rev. Lett.* **88**, 197001 (2002); P. Samuelsson and M. Büttiker, *ibid.* **89**, 046601 (2002).
- ²⁵ F. Taddei and R. Fazio, *Phys. Rev. B* **65**, 134522 (2002).
- ²⁶ E.G. Mishchenko, *Phys. Rev. B* **68**, 100409 (2002).
- ²⁷ C.J. Lambert, J. Koltai, and J. Cserti, in *Towards the Controllable Quantum States* (Mesoscopic Superconductivity and Spintronics), edited by H. Takayanagi and J. Nitta (World Scientific, Singapore, 2003), pp. 119-125.